URSI GASS 2021, Rome, Italy, 28 August - 4 September 2021

A Multifunctional SIW Filter Based Interweave and Underlay Cognitive Radio System

Sreenath Reddy Thummaluru[(1)] and Raghvendra Kumar Chaudhary[(2)]
Department of Electronics Engineering, Indian Institute of Technology (ISM) Dhanbad, Dhanbad-826004, India
[(1)]sreenath966@gmail.com and [(2)]raghvendra@iitism.ac.in

Abstract

This paper presents the design of a multifunctional SIW filter and how it will be used for designing the cognitive radio system has been explained. The frequency band concentrated here is 2.3-4.2 GHz, where multiple countries have shown their interest in mid-band 5G network implementation. The proposed SIW filter can be operated in two phases. In one phase, it acts like a tunable bandpass filter through which spectrum interweave cognitive radio functionality has been achieved. In another phase, it works like a tunable bandstop filter from which spectrum underlay cognitive radio functionality has been obtained. After developing the SIW filter, a four-port wideband MIMO antenna has been designed, which gives good isolation between the ports, envelope correlation coefficient, and antenna performance. Finally, the SIW filter has been integrated with the four-port MIMO antenna to develop the final design.

1 Introduction

The multiple input multiple output (MIMO) technology offers higher data rates, whereas the cognitive radio (CR) technology improves the spectrum efficiency. It was expected that the combination of these two technologies would be used in future communications like 5G. Combining the MIMO and CR technologies is not a new thing; it was already discussed in [1-4]. Based on the functionality, there exist two types of CR: Interweave and Underlay. This paper aim is to achieve both interweave and underlay CR functionalities using a single antenna/filtenna system. To develop such a system, we require a tunable bandpass filtenna, wideband antenna, and tunable band-reject filtenna on the same substrate. In [1, 2], both interweave and underlay CR have been designed using a single port. However, in [1, 2], a sensing antenna is also designed using that same single port. Because of this, sensing and communicating antennas (either interweave or underlay) cannot work simultaneously; thereby, the applications are limited. In [3, 4], only interweave CR has been designed. In all MIMO CR papers available in the literature [1-4], it can be found that to design a communicating antenna, either a reconfigurable filter has been introduced in the microstrip line part of an antenna or directly lumped elements are introduced in the antenna radiator section. Now consider the first case, i.e., reconfigurable patch filter in the microstrip line part of an antenna. Generally, microstrip filters have low Q-factor, which leads to high losses and thus reducing the total efficiency of the antenna. Also, many lumped elements are required for achieving the reconfigurability function, which further increases the overall losses. Coming to the second case, with the direct involvement of lumped elements in the radiator part, the far-field parameters will be largely impacted. The latter case also involves many losses and thus decreasing the overall efficiency of the antenna system. The solution is to replace the microstrip filters with high Q-factor substrate integrated waveguide (SIW) filters. However, to satisfy our requirements, a multifunctional SIW filter that can give both tunable bandpass and tunable band-reject properties simultaneously is required. In the literature, many SIW tunable filter based papers can be found. Out of them, some of the frequency tunable SIW filters can be found in [5-7]. The designs shown in [5-7] provide either bandpass or band-reject filter properties. As per the author's knowledge, no single SIW filter design available in the literature that offers both tunable bandpass and tunable band-reject properties. In this paper, such a multifunctional SIW filter has been designed, and its details can be found in section 2.

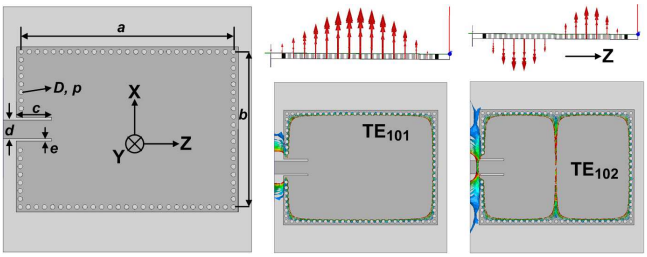

Figure 1. Center coupled SIW resonator. (a) Design with dimensions. E-field distribution at (b) first and (c) second resonant frequency (a = 44.6, b = 32.6, c = 7.4, d = 4, e = 0.5, D = 1, p = 1.7, all dimensions are in mm).

2 Design Details of SIW Filter

The design procedure starts with the center coupled SIW resonator, as shown in Fig. 1(a). The substrate we considered is Rogers RT/duroid 5880. The dimensions D and p that are shown in Fig. 1(a) represent via diameter and distance between two via centers, respectively. These two dimensions are chosen as per the SIW design rules to minimize leakage losses. The cavity dimensions are selected in such a way that the first resonant frequency of the cavity falls in between the 2.3-4.2 GHz range. The calculated first and second resonant frequencies are 3.89 GHz and 5.53 GHz, respectively. As expected, the first

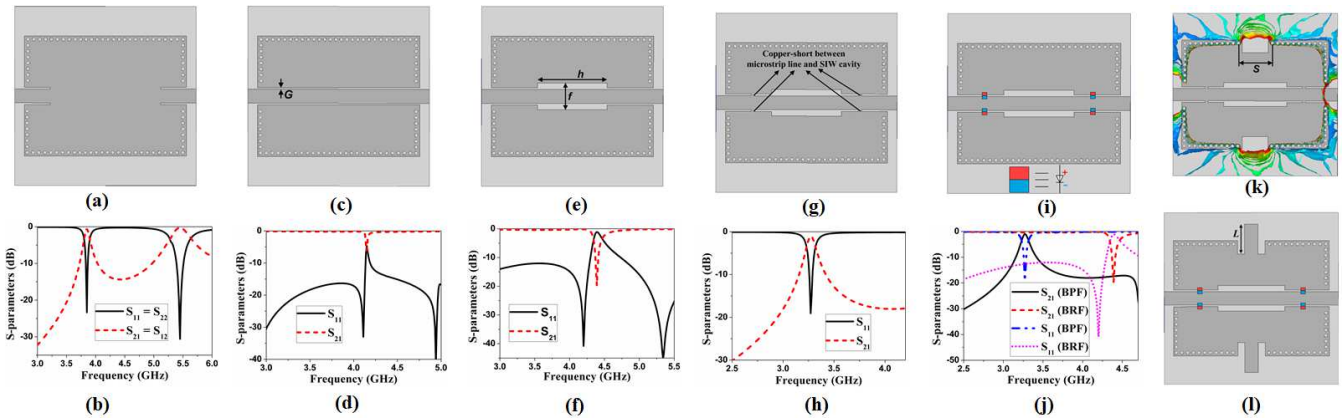

Figure 2. (a) SIW band-pass filter and its (b) S-parameters. (c) SIW cavity around microstrip line and its (d) S-parameters. (e) SIW band-reject filter and its (f) S-parameters. (g) SIW bandpass filter having conducting paths between the microstrip line and cavity, and its (h) S-parameters. (i) SIW filter having PIN diodes in place of conducting paths and its (j) S-parameters. (k) E-field distribution at first resonant frequency of SIW filter having apertures. (l) SIW filter having stubs within the apertures (G = 0.5, h = 20, f = 7.6, S = 10.7, all in mm).

two resonating modes are TE_{101} and TE_{102}. The E-field distributions of these two modes are shown in Figs. 1(b) and 1(c). The SIW resonator shown in Fig. 1(a) has been modified by adding another center-coupling port, as shown in Fig. 2(a). Now the modified design acts as a bandpass filter with the first and second bandpass frequencies are due to the first and second resonant SIW modes, respectively, as shown in Fig. 2(b). It must be noted that we designed the SIW cavity in such a way that the first bandpass frequency falls in our desired frequency range of 2.3-4.2 GHz. Now, a SIW cavity is placed around a microstrip line without any contact by leaving gap G, as shown in Fig. 2(c). This arrangement results in a coupling between the microstrip line and SIW cavity. The SIW cavity resonant mode decides the coupling frequency. Because of the coupling between the microstrip line and SIW cavity, the EM wave enters from the microstrip line to SIW cavity at the resonant frequency. This results in a band-reject response, as shown in Fig. 2(d), but with less attenuation of 8 dB. The attenuation of the stopband can be increased by enhancing the coupling, which can be done using a step impedance method [8]. The step impedance method involves the high and low impedance sections to enhance the line to cavity coupling, as shown in Fig. 2(e). With this arrangement, the attenuation of the stopband has been increased from 8 dB to 20 dB, as shown in Fig. 2(f). Involving the conducting paths between the microstrip line and SIW cavity changes the band-reject response to bandpass, as shown in Fig. 2(g). Its bandpass response is shown in Fig. 2(h). With the involvement of conducting paths, the design shown in Fig. 2(g) behaves like the one shown in Fig. 2(a). From this information, we can get an idea of how to switch between the band-reject filter and bandpass filter. Now the conducting paths have been replaced by the PIN diodes, as shown in Fig. 2(i). It can be noticed from Fig. 2(j) that when PIN diodes are ON, the SIW filter gives a bandpass response, and if PIN diodes are OFF, then the SIW filter is giving a band-reject response. The next step is to make both the bandpass and band-reject responses tunable over frequency. To achieve that, two S sized apertures are formed on the SIW cavity, as shown in Fig. 2(k). Because of these apertures, the leakage losses are increased (see the E-field distribution plot of Fig. 2(k)) and reduces the Q-factor from 707 to 684. The amount of leakage depends on the size S. If it grows, then losses increase, and Q-factor reduces. Within these apertures, a stub of length L has been placed, as shown in Fig. 2(l). It has been observed that for PIN diodes ON case, bandpass response of SIW filter becomes frequency tunable by varying the stub length (results are not shown here). Similarly, for the PIN diodes OFF case, the band-reject response of SIW filter becomes frequency tunable by changing the stub length. For S = 10.7, the tunable ranges of bandpass and band-reject responses are 100 MHz and 350 MHz, respectively. These tunable ranges can be increased by increasing the aperture size S. However, with the increase in aperture size, losses will be increased, and the Q-factor will be reduced. If we want high tuning ranges, then Q-factor should be sacrificed. Even though the Q-factors are decreasing here, they are still very much higher than the Q-factors of conventional microstrip filters.

Table I. The SIW filter operating frequencies at different V_1 voltages by fixing V_2 = 10V

V_1 voltage	Diodes status	bandpass frequency	band-reject frequency
V_1= 10V	D_2, D_3, D_4 AND D_5 OFF	3.09 GHz	3.6 GHz
V_1= 9V	D_2 ON AND D_3, D_4, D_5 OFF	3.04 GHz	3.45 GHz
V_1= 8V	D_2, D_3 ON AND D_4, D_5 OFF	2.98 GHz	3.32 GHz
V_1= 7V	D_2, D_3, D_4 ON AND D_5 OFF	2.9 GHz	3.13 GHz
V_1= 0V	D_2, D_3, D_4, D_5 ON	2.76 GHz	NA

The stubs present in Fig. 2(l) have been replaced with PIN diodes (D_2, D_3, D_4 and D_5) in Fig. 3(a), which is also our fabricated SIW filter. By controlling these PIN diodes, the bandpass and band-reject frequency can be controlled. The PIN diode model used here is BAR64-02V and its ON and OFF positions can be controlled using a biasing circuit, which is shown in Fig. 3(b). The resistor and inductor values are 2.1 kΩ (Panasonic) and 1 nH (TDK's MHQ0402PSA), respectively. The diode D_1 is used to switch the filter functionality between bandpass and band-reject. The voltages V_2 and V_3 are used to control the

diode D_1 status. Once the bandpass or band-reject functionality is achieved, the filter operating frequency can be varied by changing the status of the diodes D_2, D_3, D_4, and D_5. To control these diodes, the voltages V_1 and V_2 are used. In fact, V_2 is kept constant at 10 volts and V_1 is varied to change these diodes states between ON and OFF. More details on how to control the diodes D_1 to D_5 are given in Table I. For different PIN diode switching conditions, the measured S_{21} response for bandpass and band-reject filter cases are shown in Figs. 3(c) and 3(d), respectively. The measured frequency tunable ranges of bandpass and band-reject filters are 2.79-3.11 GHz and 3.2-3.6 GHz, respectively. Please note that these tunable ranges lie in our desired frequency range of 2.3-4.2 GHz.

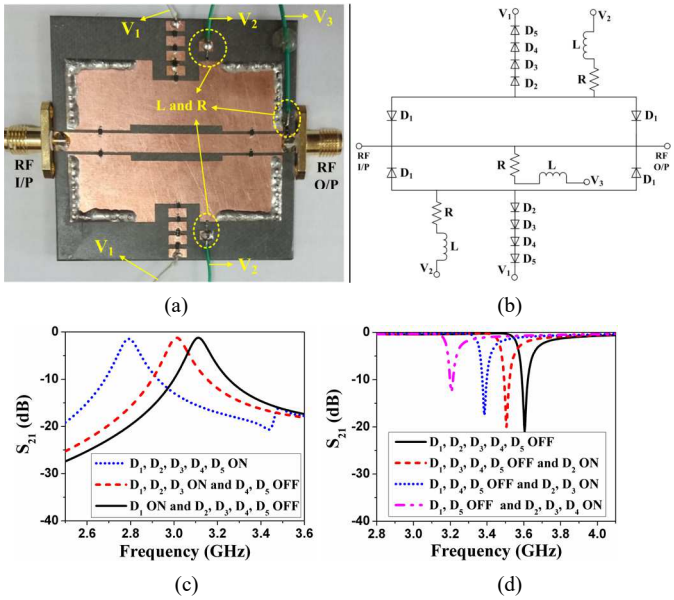

Figure 3. The fabricated SIW filter. (a) Design and (b) biasing circuit. The measured S_{21} at different switching conditions for (c) bandpass filter case and (d) band-reject filter case.

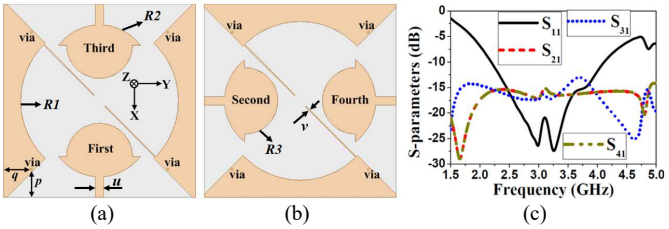

Figure 4. Four-port wideband MIMO antenna design. (a) Top view (b) bottom view, and (c) simulated *S*-parameters (p = 13.1, q = 12.5, u = 4, v = 0.5, $R1$ = 37, $R2$ = 24, $R3$ = 15.5, all in mm).

3 Integration of Filter and MIMO Antenna

In this section, the SIW filter is integrated with the four-port wideband MIMO antenna to develop the final MIMO CR system. The top and bottom views of the designed four-port wideband MIMO antenna are shown in Figs. 4(a) and 4(b), respectively. Its *S*-parameters are shown in Fig. 4(c). It can be noticed that the 10 dB impedance bandwidth of antennas is 2.3-4.2 GHz, which is our desired frequency range to develop the MIMO CR system. From Fig. 4(c), the minimum isolation between the antenna elements is around 14 dB, which is acceptable. The second and fourth antenna elements are shifted to the bottom side of the substrate to maintain less correlation between the radiated signals of adjacent antenna elements. Hence, the achieved envelope correlation coefficient (ECC) values are well below the acceptable limit of 0.5.

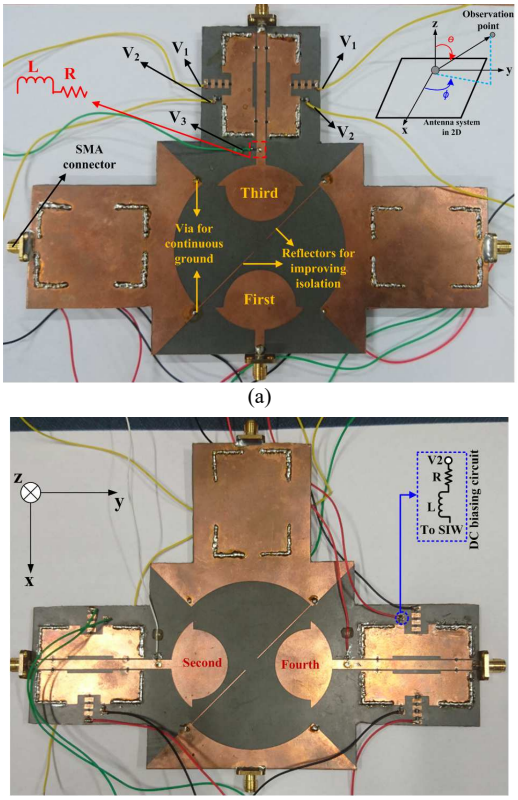

Figure 5. Final fabricated SIW filter based MIMO CR antenna system. (a) Top view and (b) bottom view.

In the next step, the SIW filter is integrated with the four-port MIMO antenna. The top and bottom views of the final integrated design are shown in Figs. 5(a) and 5(b), respectively. Except for the first port, the remaining ports of a MIMO antenna are combined with the SIW filter. After integration, the first port acts as a sensing antenna and scans the frequency range from 2.3-4.2 GHz. The measured input reflection coefficient of a sensing antenna is shown in Fig. 6(a). During the scanning, the sensing antenna identifies the spectrum holes available in the scanning range, which are not using by the primary users. Using this information, the CR allows the secondary users to communicate over these spectrum holes by using communicating antennas, thus increasing the spectrum efficiency. The second, third and fourth ports of the MIMO CR system that are indicated in Figs. 5(a) and 5(b) act like communicating antennas for both types of CR, based on diode D_1 status. If D_1 is ON, then the three ports behave like communicating antennas for interweave CR. If D_1 is OFF, then the three ports behave like communicating antennas for underlay CR. To control the diode ON and OFF states, a DC biasing network has been

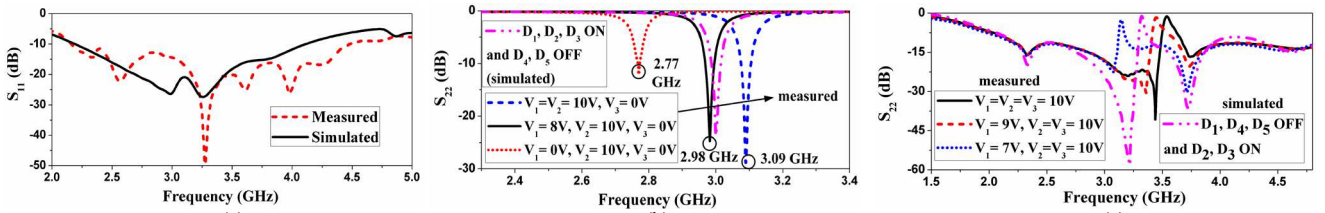

(a) (b) (c)

Figure 6. Measured input reflection coefficient, in magnitude (dB) for (a) sensing antenna when the first port is excited, (b) spectrum interweave antenna when the second port is excited, and (c) spectrum underlay antenna when the second port is excited.

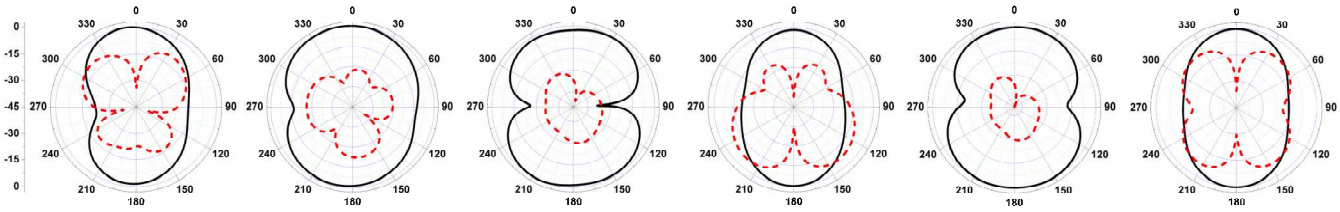

(a) (b) (c) (d) (e) (f)

Figure 7. Measured 2D radiation patterns of sensing antenna in (a) XZ-plane and (b) YZ-plane, interweave antenna in (c) XZ-plane and (d) YZ-plane, and underlay antenna in (e) XZ-plane and (f) YZ-plane (all patterns are measured and smoothened at 2.98 GHz with solid and dashed lines indicate co- and cross-polarizations.

implemented on the PCB itself, as shown in Fig. 5(b). The DC biasing voltages are represented with notations V_1, V_2, and V_3, which are shown in Fig. 5(a). If V_2 is more than V_3 by 0.82 V, then the diodes D_1 turn ON and the three ports behave like an interweave CR communicating antennas. Further, to tune the frequency of interweave CR communicating antenna, the diodes D_2 to D_5 need to be controlled which can be possible by varying V_1 voltage. At some V_1 values, the input reflection coefficient of the interweave CR communicating antenna is shown in Fig. 6(b) when second port is excited. The same input reflection coefficient can be obtained when either third or fourth port is excited. Similarly, by keeping V_2 equals to V_3 (D_1 diodes turn OFF) and by controlling V_1 voltage, the tunable frequency property of underlay CR communicating antenna has been achieved, as shown in Fig. 6(c). The interweave CR communicating antenna tunes to five different bandpass frequencies based on V_1 voltage. At all five frequencies, the radiation patterns of interweave CR communicating antenna were measured and found consistency in both *XZ*- and *YZ*-planes, which is another advantage of the proposed system. To observe the cross-polarization effect, the radiation patterns of sensing antenna, interweave and underlay CR communicating antennas are measured at 2.98 GHz, and they are shown in Fig. 7. For all three antennas in both the planes, the observed minimum difference between co- and cross-polarization in broad-side direction is around 30 dB, which is more than enough for successful communication.

4 Conclusion

The design of a CR system often involves many lumped elements that can make system more lossy. Hence, it is difficult to design the highly efficient CR system using the conventional microstrip filters. In this paper, for the first time, we came up with an idea of designing the CR system using SIW filter. Even with the involvement of many lumped elements, the presented SIW filter still gives us the Q-factors of around 600 which makes it more suitable for designing CR system. In addition, the presented SIW filter is working like either tunable bandpass filter or tunable band-reject filter which given us the advantage of achieving both interweave and underlay CR functionalities using a single design. Once integrating the SIW filter with four-port MIMO antenna, the final design is giving good far-field, MIMO, and CR performance, which makes it ideal candidate for interweave and underlay CR applications.

5 References

1. S. R. Thummaluru, M. Ameen, and R. K. Chaudhary, "Four-Port MIMO Cognitive Radio System for Mid-Band 5G Applications," *IEEE Transactions on Antennas and Propagation*, **67**, 8, August 2019, pp. 5634-5645, doi:10.1109/TAP.2019.2918476.
2. T. Alam, S. R. Thummaluru, and R. K. Chaudhary, "Integration of MIMO and Cognitive Radio for Sub-6 GHz 5G Applications," *IEEE Antennas and Wireless Propagation Letters,* **18**, 10, October 2019, pp. 2021 - 2025, doi: 10.1109/LAWP.2019.2936312.
3. R. Hussain, M. S. Sharawi, and A. Shamim, "An Integrated Four-Element Slot-Based MIMO and a UWB Sensing Antenna System for CR Platforms," *IEEE Transactions on Antennas and Propag*ation, **66**, 2, Febraury 2018, pp. 978-983, doi:10.1109/TAP.2017.2781220.
4. Y. Tawk, J. Costantine, and C. G. Christodoulou, "Reconfigurable filtennas and MIMO in cognitive radio applications," IEEE Transactions on Antennas and Propagation, **62**, 3, March 2014, pp. 1074-1083, doi: 10.1109/TAP.2013.2280299.
5. V. Sekhar, M. Armendariz, and K. Entesari, "A 1.2–1.6-GHz Substrate-Integrated-Waveguide RF MEMS Tunable Filter," *IEEE Transactions on Microwave Theory and Techniques*, **59**, 4, April 2011, pp. 866–876, doi:10.1109/TMTT.2011.2109006.
6. A. Anand, J. Small, D. Peroulis, and X. Li, "Theory and Design of Octave Tunable Filters With Lumped Tuning Elements," *IEEE Transactions on Microwave Theory and Techniques*, **61**, 12, December 2013, pp. 4353–4364, doi: 10.1109/TMTT.2013.2287674
7. B. Lee, B. Koh, S. Nam, T. –H. Lee, and J. Lee, "Band-Switchable Substrate-Integrated Waveguide Resonator and Filter," *IEEE Transactions on Microwave Theory and Techniques*, **66**, 1, January 2018, pp. 147-156, doi: 10.1109/TMTT.2017.2737989.
8. Ian C. Hunter, "Theory and Design of Microwave Filter," *The Institution of Electrical Engineers*, 2001, doi: 10.1049/PBEW048E.